Available online at www.sciencedirect.com

ScienceDirect

Procedia IUTAM 12 (2015) 93 – 104

Procedia IUTAM

www.elsevier.com/locate/procedia

IUTAM Symposium on Mechanics of Soft Active Materials

2D mixed hybrid FEM of Lanir model

Cong Yu[a], Jacques M.Huyghe[a,*], Kamyar Malakpoor[a]

[a]*Eindhoven Univeristy of Technology, Eindhoven 5600MB, the Netherlands*

Abstract

Osmoelastic media have large negatively charged groups attached to the solid matrix. Due to the fixed charges, the total ion concentration inside the medium is higher than in the surrounding fluid. This excess of ion particles leads to an osmotic pressure difference, which causes swelling of the medium. Lanir's osmoelastic model assumes that small ions are always in equilibrium with the external salt concentration. This means that ion contribution is neglected and the medium is described by two constituents only: the solid and the fluid. In this paper, we implemented Lanir model using MHFEM (Mixed Hybrid Finite Element Method) for consolidation experiment in both 1D and 2D cases, with result verification with analytical solution in 1D. The constituents are assumed to be incompressible. Infinitesimal deformations are assumed. The material is linear elastic, isothermal, isotropic, homogeneous and fully saturated.

Peer-review under responsibility of Konstantin Volokh and Mahmood Jabareen.

Keywords: Osmotic swelling; Consolidation; Lanir model; Linear elasticity; Mixed hybird finite element method;

1. Introduction

Super absorbent polymer has been widely used in industry, for example in the diapers. Such super absorbent polymers are ionic polymers. Thus when the super absorbent submerged in the salt solution, besides simply mixing, the sodium ions move freely within the network and contribute to the osmotic pressure within the gel.

Gels can exhibit significant swelling and shrinking behaviour when in contact with salt concentrations. This phenomena observed in gels is caused by the electric charges fixed to the solid. These charges result in various features, including swelling, electro-osmosis, streaming potentials and streaming currents. We differentiate between the components and phases in such a way that the components are considered to be continua with macroscopic properties.In our case, there are two components involved. Namely, fluid and solid. Mixture theory[1] provides us a framework, where mechanical deformations and diffusion convection and chemical reactions are integrated.

From the earlier work in geomechanics Biot[2] presented a biphasic model which describes the mathematical and physical consequences of three dimensional consolidation. Lanir[3] extended the Biot model for incompressible constituents, namely the solid matrix and interstitial fluid, by including Donnan osmotic pressure, but neglecting the influence of ion flow. Lai et al.[4] extended Lanirs model to the triphasic theory including ionic diffusion-convection. Huyghe and Janssen[5] developed an electro-chemomechanical model using four constituents.

* Corresponding author. Tel.: +31-40-247-3137 ; fax: +0-000-000-0000.
E-mail address: J.M.R.Huyghe@tue.nl

Peer-review under responsibility of Konstantin Volokh and Mahmood Jabareen.
doi:10.1016/j.piutam.2014.12.011

Gu et al.[6] developed a multiionic model. van Loon et al.[7] implemented a 3D Finite Element model of the quadriphasic model. Meerveld et al.[8] validated the quadriphasic model by analytical solutions. The confined and unconfined compression tests are common validation tools.Wilson et al.[9] compared the biphasic swelling model[3] with the quadriphasic model[5] and showed that the flow of ions indeed influences the pathway to equilibrium with the external fluid.Kamyar[10] simulated both consolidation and free swelling experiment assuming quadraphisic model using mixed and hybrid FEM with the validation in one dimensional space Although the mechano-electro-chemical models are more realistic in transient behavior, Lanirs model is a reliable approximation for the modeling of ionized porous media at a constant external salt concentration.

Although Lanir model has been incorporated in the commercial software Abaqus, it has not been implemented using mixed hybrid FEM. In this paper we use mixed and hybrid FEM for Lanir model for small deformation. We did consolidation experiments in both 1D and 2D case, with result verification in 1D with analytical solutions.

2. Lanir model

Due to the fixed charges, the total ion concentration inside the medium is higher than in the surrounding fluid. This excess of ion particles leads to an osmotic pressure difference, which causes swelling of the medium. Lanir's osmoelastic model assumes that small ions are always in equilibrium with the external salt concentration. This means that ion contribution is neglected and the medium is described by two constituents only: the solid and the fluid. The constituents are assumed to be incompressible. The material is linear elastic, isothermal, isotropic, homogeneous and fully saturated.In this section, we will present the Lanir model and its linearization in terms of governing equations in the consolidation case.

2.1. Governing equations

Osmotic swelling is included by the introduction of the chemical potential of the fluid, which is a measure for the free energy of the fluid. The chemical potential of the fluid μ is defined per unit volume fluid and commits the following expression:

$$\mu = \mu_0 + p - \pi, \tag{1}$$

where p denotes the hydrostatic pressure and π the osmotic pressure and μ_0 denotes the reference chemical potential. We set

$$\mu_0 = 2RTc_{out}, \tag{2}$$

where R, T are the universal gas constant and the absolute temperature respectively and c_{out} denotes the ions concentration in the outer solution.

Thus the governing equations are comprised of three equations, containing the conservation of total momentum, total mass conservation and a modified Darcy's law, which are expressed as:

$$\nabla \cdot \boldsymbol{\sigma} = \mathbf{0}, \tag{3}$$

$$\frac{\partial \nabla \cdot \boldsymbol{u}}{\partial t} + \nabla \cdot \boldsymbol{q} = 0, \tag{4}$$

$$\boldsymbol{q} = -K\nabla\mu. \tag{5}$$

Note that $\boldsymbol{u}$ is the displacement field, $\boldsymbol{q}$ is the fluid flow and K is a constant representing permeability and $\boldsymbol{\sigma}$ denotes the total stress, which for a porous media commits the following expression:

$$\boldsymbol{\sigma} = \boldsymbol{\sigma}_e - p\boldsymbol{I} + \sigma_0\boldsymbol{I}, \tag{6}$$

where $\sigma_0\boldsymbol{I}$ is the pre-stress existing in the gel due to the initial osmotic pressure and is calculated as:

$$\sigma_0 = \pi(x, y, 0) - \mu_0. \tag{7}$$

σ_e denotes the effective stress and for a isotropic linear elastic material, it can be written as:

$$\boldsymbol{\sigma}_e = 2\mu_s\boldsymbol{\mathcal{E}} + \lambda_s tr(\mathcal{E})\boldsymbol{I}, \tag{8}$$

where μ_s and λ_s are Lam constant and $\mathcal{E}$ is the linearized strain tensor. In Lanir model, the osmotic pressure π is expressed as:

$$\pi = RT\Gamma(c^+ + c^-), \tag{9}$$

$$c^+ + c^- = \sqrt{(c^{fc})^2 + 4(c_{out})^2}, \tag{10}$$

$$c^{fc} = c_0^{fc}\frac{\varphi_0}{\varphi_0 + \nabla \cdot \boldsymbol{u}}. \tag{11}$$

where Γ is the osmotic coefficient of the ions and assumed to be constant.c^+, c^-, c^{fc} denotes the current cation and anion and fixed charge molar concentration respectively. In (11), c_0^{fc} and φ_0 denote the fixed charge concentration and porosity in the initial state. Also from (11) we can see that $\pi, c^f c$ and so on are nonliear functions of $\boldsymbol{u}$.

To solve the problem analytically, we linearize the osmotic pressure term π. Due to small deformation assumption, the linearization around the initial strain makes sense. We can linearize this term as follows:

$$\begin{aligned}\pi &= \pi|_{\mathcal{E}_0} + \frac{\partial \pi}{\partial \boldsymbol{\mathcal{E}}}|_{\mathcal{E}_0} : (\boldsymbol{\mathcal{E}} - \boldsymbol{\mathcal{E}_0}) \\ &= RT\Gamma(C_0 - \nabla \cdot \boldsymbol{u}C_1),\end{aligned}$$

where

$$C_0 = \sqrt{(c_0^{fc})^2 + 4(c_{out})^2}, \tag{12}$$

$$C_1 = \frac{(c_0^{fc})^2}{(\varphi_0 + \mathcal{E}_0)C_0}. \tag{13}$$

Note that the initial strain $\mathcal{E}_0$ is calculated according to the initial stress σ_0 and the linear elasticity constitutive law. Thus, in 2D case,

$$\mathcal{E}_0 = \frac{\sigma_0}{\mu_s + \lambda_s}\boldsymbol{I}. \tag{14}$$

2.2. Configuration of the consolidation experiment

As shown in Fig.1, the sample is placed on a glass filter with a piston applying force above and the sample is only allowed to move in the vertical direction.

2.3. Boundary and initial conditions for consolidation experiment

Based on the experimental set-up, this is essentially a 1D problem but in 2D configuration. Our domain of interest is $[0, L] \times [0, L]$. At $t = 0^+$, we apply the force $-f_0$ via the piston. Since the bottom side of the sample ($y = 0$) is in contact of the fluid (through the glass filter), we have:

$$\boldsymbol{u}(x, 0, t) = \boldsymbol{0}, \quad \forall x \in [0, L] \tag{15}$$

$$u_1(0, y, t) = 0, \quad \forall y \in [0, L] \tag{16}$$

$$u_2(L, y, t) = 0, \quad \forall y \in [0, L] \tag{17}$$

$$\mu(x, 0, t) = 0, \quad \forall x \in [0, L]. \tag{18}$$

At the top and left and right sides ($y = L$ and $x = 0, L$), since there is no flow in or out of the sample, we have

$$\frac{\partial \mu}{\partial y}(x, L, t) = 0, \quad \forall x \in [0, L],$$

$$\frac{\partial \mu}{\partial x}(0, y, t) = 0, \quad \forall y \in [0, L],$$

$$\frac{\partial \mu}{\partial x}(L, y, t) = 0, \quad \forall y \in [0, L],$$

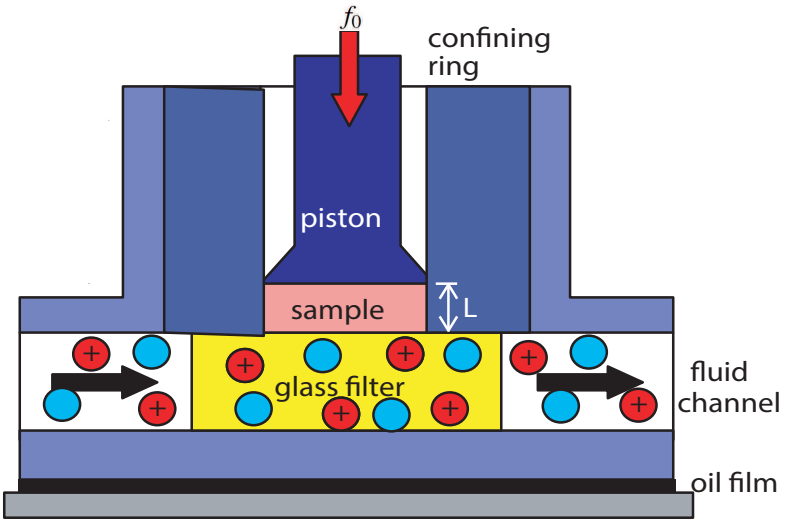

Fig. 1. Schematic representation of the experimental set-up

The application of the force reflected in the boundary condition can be expressed as:

$$\boldsymbol{\sigma} = \boldsymbol{F}_0 = \begin{pmatrix} 0 & 0 \\ 0 & -f_0 \end{pmatrix}, \tag{19}$$

As we assume incompressibility of the fluid and solid, the instantaneous response of the gel is:

$$\mu(x, y, t = 0^+) = f_0, \tag{20}$$

$$\boldsymbol{u}(x, y, t = 0^+) = \boldsymbol{0}. \tag{21}$$

This indicates that instantaneously the fluid undergoes an overpressurization, and then gradually the overpressure disappears due to the diffusion process and consequently the solid and the fixed charges progressively sustain the loading alone.

3. Mixed Hybrid Finite Element Methods

MHFEM is a modified finite element method. It has two distinctive aspects: it takes the mixed formulation and it introduces a Lagrangian multiplier λ which facilitates solving the resulting linear system. In this section, we will present step by step how we apply MHFEM to our system of equations. The verification of this method with the analytical solution will be given in the next section.

3.1. Weak formulations

To employ finite element method, we need to first derive its weak formulations. Note that even in the strong form we have adopted the mixed formulation by setting the flow q as an independent variable.The weak formulation corresponding to the governing equations (strong form) is:

Find $(\boldsymbol{u}, \boldsymbol{q}, \mu) \in (\mathcal{V}(\Omega) \times H(div; \Omega) \times \mathcal{W}(\Omega))$, such that for any $(\bar{\boldsymbol{u}}, \bar{\boldsymbol{q}}, \bar{\mu}) \in (\mathcal{V}(\Omega) \times H(div; \Omega) \times \mathcal{W}(\Omega))$, satisfy

$$\int_\Omega (2\mu_s \mathcal{E}(\boldsymbol{u}) : \mathcal{E}(\bar{\boldsymbol{u}}) + \lambda_s \nabla \cdot \boldsymbol{u} \nabla \cdot \bar{\boldsymbol{u}})\, d\Omega - \int_\Omega \nabla \cdot \bar{\boldsymbol{u}} \mu\, d\Omega = \int_\Omega (\pi(c^{fc}) - \mu_0 - \sigma_0) \nabla \cdot \bar{\boldsymbol{u}}\, d\Omega - \int_{\Gamma_T} \boldsymbol{F}_0 \boldsymbol{n} \cdot \bar{\boldsymbol{u}} d\Gamma, \tag{22}$$

$$-\frac{\partial}{\partial t} \int_\Omega \nabla \cdot \boldsymbol{u} \bar{\mu}\, d\Omega - \int_\Omega \nabla \cdot \boldsymbol{q} \bar{\mu}\, d\Omega = 0, \tag{23}$$

$$\frac{1}{K} \int_\Omega \boldsymbol{q} \cdot \bar{\boldsymbol{q}}\, d\Omega - \int_\Omega \nabla \cdot \bar{\boldsymbol{q}} \mu\, d\Omega = 0. \tag{24}$$

The equations can be rewritten as:

$$a(\boldsymbol{u}, \bar{\boldsymbol{u}}) + b(\bar{\boldsymbol{u}}, \mu) = f(\bar{\boldsymbol{u}}), \tag{25}$$

$$c(\boldsymbol{q}, \bar{\boldsymbol{q}}) + d(\boldsymbol{q}, \bar{\mu}) = 0, \tag{26}$$

$$\frac{\partial}{\partial t} b(\boldsymbol{u}, \bar{\mu}) + d(\bar{\boldsymbol{q}}, \mu) = 0, \tag{27}$$

where

$$a(\boldsymbol{u}, \bar{\boldsymbol{u}}) = \int_\Omega (2\mu_s \mathcal{E}(\boldsymbol{u}) : \mathcal{E}(\bar{\boldsymbol{u}}) + \lambda_s \nabla \cdot \boldsymbol{u} \nabla \cdot \bar{\boldsymbol{u}})\, d\Omega, \tag{28}$$

$$b(\boldsymbol{u}, \bar{\mu}) = -\int_\Omega \nabla \cdot \boldsymbol{u} \bar{\mu}\, d\Omega, \tag{29}$$

$$c(\boldsymbol{q}, \bar{\boldsymbol{q}}) = \frac{1}{K} \int_\Omega \boldsymbol{q} \cdot \bar{\boldsymbol{q}}\, d\Omega, \tag{30}$$

$$d(\bar{\boldsymbol{q}}, \mu) = -\int_\Omega \nabla \cdot \bar{\boldsymbol{q}} \mu\, d\Omega, \tag{31}$$

$$f(\bar{\boldsymbol{u}}) = \int_\Omega (\pi(c^{fc}) - \mu_0 - \sigma_0) \nabla \cdot \bar{\boldsymbol{u}}\, d\Omega - \int_{\Gamma_T} \boldsymbol{F}_0 \boldsymbol{n} \cdot \bar{\boldsymbol{u}} d\Gamma. \tag{32}$$

The function spaces are defined as

$$\mathcal{V}(\Omega) = \{u \in (H^1(\Omega))^2 | u = 0, \text{on } \Gamma_D\},$$
$$H(div; \Omega) = \{q \in L^2(\Omega) | \nabla \cdot q \in L^2(\Omega), q \cdot n = 0, \text{ on } \Gamma_D\},$$
$$\mathcal{W}(\Omega) = \{\mu \in (L^2(\Omega))^2 |\, \mu = 0, \text{on } \Gamma_B\},$$

where Γ_T denotes the top side of the sample where the force is applied by the piston and Γ_B denotes the bottom side of the sample and Γ_D denotes the boundary wherever commits the Dirichlet boundary condition for $\boldsymbol{u}$.

3.2. Function spaces and their basis functions

Next, we move to the spatial discretization method. Here we use mixed finite element method. The approximation space of the function spaces are:

$$\boldsymbol{u}_h \in (P_0^1(\mathcal{T}_h))^2, \tag{33}$$

$$\boldsymbol{q}_h \in RT_0^0(\mathcal{T}_h), \tag{34}$$

$$\mu_h \in M_{-1}^0(\mathcal{T}_h), \tag{35}$$

where

$$(P_0^1(\mathcal{T}_h))^2 = P_{-1}^1(\mathcal{T}_h) \cap H^1(\Omega), \tag{36}$$

$$P_{-1}^1(\mathcal{T}_h) = \{\varphi \in L^2(\Omega) : \varphi|_T \in P^1(T), \quad \forall T \in \mathcal{T}_h\}, \tag{37}$$

$$RT_0^0(\mathcal{T}_h) = RT_{-1}^0(\mathcal{T}_h) \cap H(div; \Omega), \tag{38}$$

$$RT_{-1}^0(\mathcal{T}_h) = \{v \in L^2(\Omega) : v|_T \in RT^0(T), \quad \forall T \in \mathcal{T}_h\}, \tag{39}$$

$$M_{-1}^0(\mathcal{T}_h) = \{\psi \in L^2(\Omega) : \psi|_T \in M^0(T), \quad \forall T \in \mathcal{T}_h\}. \tag{40}$$

Note that $P^1(T)$ denotes the space of polynomials of degree less or equal than one and $RT^0(T)$ is defined as

$$RT^0(T) = \{(a + bx, c + by), a, b, c \in \mathbb{R}\}, \tag{41}$$

$M^0(T)$ denotes the space of constant function on T and $\mathcal{T}_h$ is certain regular triangulation of the domain Ω, . We select quadrilaterals to be our elements. We need to know the basis functions of the approximation space. To do so, we first introduce the isoparametric concept.

Firstly, we define reference element in the parent domain. The coordinates in the parent domain are with hat namely $(\hat{x}, \hat{y})$. In this case, the parent domain is a square with four nodes: $\hat{x}_1, \hat{x}_2, \hat{x}_3, \hat{x}_4$.Their coordinates are $(0, 0), (1, 0), (1, 1), (0, 1)$ respectively. The basis function associated with node $\hat{x}_i$ are:

$$\begin{aligned}
\hat{\varphi}_1(\hat{x}, \hat{y}) &= (1 - \hat{x})(1 - \hat{y}),\\
\hat{\varphi}_2(\hat{x}, \hat{y}) &= (1 - \hat{x})\hat{y},\\
\hat{\varphi}_3(\hat{x}, \hat{y}) &= \hat{x}\hat{y},\\
\hat{\varphi}_4(\hat{x}, \hat{y}) &= \hat{x}(1 - \hat{y}).
\end{aligned}$$

Since we use isoparametric element, the interpolation of function u_h is written as:

$$(\boldsymbol{u}_h(\hat{x}, \hat{y}))_y = \sum_{i=1}^{4} \hat{\varphi}_i(\hat{x}, \hat{y}) u_h^i, \tag{42}$$

where $(\cdot)_y$ denotes the $y-$ component of the vector. Note that as pointed out in the experiment configuration, there is no horizontal displacement allowed which means that $(\boldsymbol{u}_h(\hat{x}, \hat{y}))_x = 0$. u_h^i denotes the displacement of the nodes i.

Secondly, we decide the basis function for the function space $RT^0(\mathcal{T}_h)$. In the parent domain the basis function can be written as:

$$\begin{aligned}
\hat{\boldsymbol{v}}_1(\hat{x}, \hat{y}) &= \begin{pmatrix} \hat{x} \\ 0 \end{pmatrix},\\
\hat{\boldsymbol{v}}_2(\hat{x}, \hat{y}) &= \begin{pmatrix} 0 \\ \hat{y} \end{pmatrix},\\
\hat{\boldsymbol{v}}_3(\hat{x}, \hat{y}) &= \begin{pmatrix} \hat{x} - 1 \\ 0 \end{pmatrix},\\
\hat{\boldsymbol{v}}_4(\hat{x}, \hat{y}) &= \begin{pmatrix} 0 \\ \hat{y} - 1 \end{pmatrix}.
\end{aligned}$$

The transformation from the parent domain to the real element is done by Piola's transformation:

$$\boldsymbol{v}_i(x, y) = (\det \boldsymbol{B}_2)^{-1} \boldsymbol{B}_2 \hat{\boldsymbol{v}}_i(\hat{x}, \hat{y}), \tag{43}$$

where $\boldsymbol{B}_2$ is calculated according to the coordinates of the elements as:

$$\boldsymbol{B}_2 = \begin{pmatrix} x_2 - x_1 & x_4 - x_1 \\ y_2 - y_1 & y_4 - y_1 \end{pmatrix}. \tag{44}$$

At last, the basis function for the function space $M^0_{-1}(\mathcal{T}_h)$ are simply step functions per element domain. Namely,

$$\psi_k(x) = \delta_{kl}, \quad x \in T_l. \tag{45}$$

3.3. The resulting linear system

With the basis functions presented above, we are able to convert the differential equations into a linear system. Suppose the total number of nodes edges and elements are I, J, K respectively.

The displacement, flux and chemical potential fields are interpolated as:

$$(\boldsymbol{u}_h(\hat{x},\hat{y},t))_y = \sum_{i=1}^{I} u_i^h(t)\varphi_i(\hat{x},\hat{y}),$$
$$\boldsymbol{q}_h(x,y,t) = \sum_{j=1}^{J} q_j^h(t)\boldsymbol{v}_j(x,y),$$
$$\mu(x,y,t) = \sum_{k=1}^{K} \mu_k^h(t)\psi_k(x,y).$$

With the relations standing above, the resulting linear system is

$$\mathfrak{A}\frac{d\boldsymbol{y}}{dt} + \mathfrak{B}\boldsymbol{y} = \mathfrak{F}, \tag{46}$$

where

$$\mathfrak{A} = \begin{pmatrix} 0 & 0\,0 \\ 0 & 0\,0 \\ \boldsymbol{B}^T & 0\,0 \end{pmatrix}, \qquad \mathfrak{B} = \begin{pmatrix} \boldsymbol{A} & 0 & \boldsymbol{B} \\ 0 & \boldsymbol{C} & \boldsymbol{D} \\ 0 & \boldsymbol{D}^T & 0 \end{pmatrix} \tag{47}$$

and

$$\boldsymbol{y} = [\tilde{\boldsymbol{u}}, \tilde{\boldsymbol{q}}, \tilde{\boldsymbol{\mu}}]^T,$$
$$\mathfrak{F} = [\boldsymbol{F}, 0, 0]^T.$$

Note that

$$\tilde{\boldsymbol{u}} = [u_1^h(t), ..., u_I^h(t)],$$
$$\tilde{\boldsymbol{q}} = [q_1^h(t), ..., q_J^h(t)],$$
$$\tilde{\boldsymbol{\mu}} = [\mu_1^h(t), ..., \mu_K^h(t)].$$

The matrices are computed as:

$$\boldsymbol{A}_{i_1 i_2} = \int_\Omega (2\mu_s \boldsymbol{\mathcal{E}}(\varphi_{i_1}) : \boldsymbol{\mathcal{E}}(\varphi_{i_2}) + \lambda_s \nabla\cdot\varphi_{i_1} \nabla\cdot\varphi_{i_2})\, d\Omega,$$
$$\boldsymbol{B}_{ik} = -\int_\Omega \nabla\cdot\varphi_i \psi_k \, d\Omega,$$
$$\boldsymbol{C}_{j_1 j_2} = \frac{1}{K}\int_\Omega \boldsymbol{v}_{j_1}\cdot\boldsymbol{v}_{j_2}\, d\Omega,$$
$$\boldsymbol{D}_{jk} = -\int_\Omega \nabla\cdot\boldsymbol{v}_j \psi_k \, d\Omega,$$
$$\boldsymbol{F}_i = \int_\Omega (\pi(c^{fc}) - \mu_0 - \sigma_0)\nabla\cdot\varphi_i \, d\Omega - \int_{\Gamma_T} \boldsymbol{F}_0 \boldsymbol{n}\cdot\varphi_i d\Gamma,$$

where $i_1, i_2, i = 1, ..., I$, $j_1, j_2, j = i, ..., J$, $k = 1, ..., K$.

3.4. Hybridization of the system

The stiffness matrix we have derived so far is indefinite and this brings trouble when we calculate the solution for our linear system. To solve this problem, we introduce the so-called "hybrid" system by introducing another variable (as Lagrangian multiplier) λ_h.

Note that the resulting element matrices derived in the last subsection assume the search and test space for $\boldsymbol{q}$ and $\bar{\boldsymbol{q}}$ as $RT^0_{-1}(\mathcal{T}_h)$ instead of $RT^0_0(\mathcal{T}_h)$. One can show that the sufficient and necessary condition for $\boldsymbol{q}_h \in RT^0_{-1}(\mathcal{T}_h)$ to be $\boldsymbol{q}_h \in RT^0_0(\mathcal{T}_h)$ is that

$$\sum_{T\in\mathcal{T}_h}\int_{\partial T}\lambda_h \boldsymbol{n}_T\cdot\boldsymbol{q}_h ds = 0, \qquad \forall\lambda_h \in M^0_{-1,D}(E_h), \tag{48}$$

where $\boldsymbol{n}_T$ is the outward normal to ∂T. Define $M^0_{-1,D}(E_h)$ as:

$$M^0_{-1,D}(E_h) = \{\lambda \in M^0_{-1}(E_h)|\ \lambda = 0 \quad \text{on}\ \ \Gamma_B\}, \tag{49}$$

$$M^0_{-1}(E_h) = \{\cup_{e\in E_h}\lambda_e|\ \lambda_e \in M^0(e), \quad \forall e \in E_h\}, \tag{50}$$

$$\tag{51}$$

where E_h denotes the collection of edges of subdomains T and $M^0(e)$ be the space of constant functions on e.

Thus the hybrid version of the mixed method with lowest-order Raviart-Thomas element reads as follows:

Find $(\boldsymbol{u}_h, \boldsymbol{q}_h, \mu_h, \lambda_h) \in (P^1_0(\mathcal{T}_h))^2 \times RT^0_{-1}(\mathcal{T}_h) \times M^0_{-1}(\mathcal{T}_h) \times M^0_{-1,D}(E_h)$, such that

$$\int_\Omega (2\mu_s\boldsymbol{\mathcal{E}}(\boldsymbol{u}_h) : \boldsymbol{\mathcal{E}}(\bar{\boldsymbol{u}}_h) + \lambda_s\nabla\cdot\boldsymbol{u}_h\nabla\cdot\bar{\boldsymbol{u}}_h)\,d\Omega - \int_\Omega \nabla\cdot\bar{\boldsymbol{u}}_h\mu_h\,d\Omega = \int_\Omega(\pi(c^{fc}) - \mu_0 - \sigma_0)\nabla\cdot\bar{\boldsymbol{u}}_h\,d\Omega - \int_{\Gamma_T}\boldsymbol{F}_0\boldsymbol{n}\cdot\bar{\boldsymbol{u}}d\Gamma, \tag{52}$$

$$\frac{1}{K}\int_\Omega \boldsymbol{q}_h\cdot\bar{\boldsymbol{q}}_h\,d\Omega - \sum_{T\in\mathcal{T}_h}(\int_T \nabla\cdot\bar{\boldsymbol{q}}_h\mu_h\,d\Omega - \int_{\partial T}\lambda_h\boldsymbol{n}_T\cdot\bar{\boldsymbol{q}}_h ds) = 0, \tag{53}$$

$$-\frac{\partial}{\partial t}\int_\Omega \nabla\cdot\boldsymbol{u}_h\bar{\mu}_h\,d\Omega - \int_\Omega \nabla\cdot\boldsymbol{q}_h\bar{\mu}_h\,d\Omega = 0, \tag{54}$$

$$\sum_{T\in\mathcal{T}_h}\int_{\partial T}\bar{\lambda}_h\boldsymbol{n}_T\cdot\boldsymbol{q}_h ds = 0, \tag{55}$$

for $(\bar{\boldsymbol{u}}_h, \bar{\boldsymbol{q}}_h, \bar{\mu}_h, \bar{\lambda}_h) \in (P^1_0(\mathcal{T}_h))^2 \times RT^0_{-1}(\mathcal{T}_h) \times M^0_{-1}(\mathcal{T}_h) \times M^0_{-1,D}(E_h)$.

Using the above hybridization procedure, one can show that the above linear system is simplified to the following problem with the number of unknowns reduced to two:

$$\begin{pmatrix}\boldsymbol{A}\tilde{\boldsymbol{u}}\\ 0\end{pmatrix} + \begin{pmatrix}\mathfrak{A}_1 & \mathfrak{A}_2\\ \mathfrak{A}_2^T & -\mathfrak{A}_3\end{pmatrix}\begin{pmatrix}\frac{d}{dt}\tilde{\boldsymbol{u}}\\ \boldsymbol{\lambda}\end{pmatrix} = \begin{pmatrix}F\\ 0\end{pmatrix}, \tag{56}$$

where

$$\boldsymbol{\lambda} = [\lambda^h_1(t), ..., \lambda^h_J(t)], \tag{57}$$

$$\mathfrak{A}_1 = \boldsymbol{B}(\boldsymbol{D^TC^{-1}D})^{-1}\boldsymbol{B^T}, \tag{58}$$

$$\mathfrak{A}_2 = -\boldsymbol{B}(\boldsymbol{D^TC^{-1}D})^{-1}\boldsymbol{D^TC^{-1}E}, \tag{59}$$

$$\mathfrak{A}_3 = -\boldsymbol{E^TC^{-1}D}(\boldsymbol{D^TC^{-1}D})^{-1}\boldsymbol{D^TC^{-1}E} + \boldsymbol{E^TC^{-1}E}, \tag{60}$$

$$\tag{61}$$

where

$$\boldsymbol{E}_{j_1,j_2} = \int_{e_{j_2}}\boldsymbol{n}\cdot\boldsymbol{v}_{j_1}ds. \tag{62}$$

3.5. Time discretization scheme

At the moment we use implicit Euler as time discretization scheme, which means that if we are now at time step n, we need to solve the following system to get the solution for the next time step.

$$\begin{pmatrix}\boldsymbol{A} + \mathfrak{A}_1/\Delta t & \mathfrak{A}_2\\ \mathfrak{A}_2^T & -\Delta t\mathfrak{A}_3\end{pmatrix}\begin{pmatrix}\tilde{\boldsymbol{u}}_{n+1}\\ \boldsymbol{\lambda}_{n+1}\end{pmatrix} = \begin{pmatrix}\boldsymbol{F} + \mathfrak{A}_1\tilde{\boldsymbol{u}}_n/\Delta t\\ \mathfrak{A}_2^T\tilde{\boldsymbol{u}}_n\end{pmatrix}. \tag{63}$$

3.6. Dealing with the osmotic pressure term

It should be noticed that till now, we always write the osmotic pressure term π to the right hand side in the force vector to keep the symmetric structure of the equations. Since the calculation of the vector F demands the value of $\pi(c^{fc})$ and therefore is function of divergence of u. We use the following iterative procedure to deal with the problem:

- Given $c_n^{fc}(= c_{n+1,(0)}^{fc})$, set $k = 0$, set criteria $\delta = 10^{-11}$.
- Calculate $u_{n+1,(k)}$ according to (63), where $c^{fc} = c_{n+1,(k)}^{fc}$
- Calculate $c_{n+1,(k+1)}^{fc}$ according to (11).
- Check the convergence: $\|c_{n+1,(k)}^{fc} - c_{n+1,(k+1)}^{fc}\| \leq \delta$.
- If it is true then $c_{n+1}^{fc} = c_{n+1,(k+1)}^{fc}$; if not, $k = k + 1$, repeat from the second step.

4. Analytical solution in one dimension

To verify the computation result using MHFEM, we also explored the analytical solution in one dimension. The governing equations and corresponding boundary conditions in consolidation experiment can be rewritten in one dimension as:

$$\frac{\partial \pi}{\partial y} = (2\mu_s + \lambda_s)\frac{\partial^2 u}{\partial y^2} - \frac{\partial \mu}{\partial y}, \tag{64}$$

$$0 = \frac{\partial^2 u}{\partial t \partial y} - K\frac{\partial^2 \mu}{\partial y^2}, \tag{65}$$

$$\pi = RT\Gamma\sqrt{(c_0^{fc}\frac{\varphi_0}{\varphi_0 + \frac{\partial u}{\partial y}})^2 + 4(c_{out}^2)} \approx RT\Gamma(C_0 - \frac{\partial u}{\partial y}C_1). \tag{66}$$

Boundary and initial conditions are specified as:

$$\mu(0,t) = 0 \quad t > 0 \tag{67}$$

$$u(0,t) = 0, \quad t \geq 0, \tag{68}$$

$$\frac{\partial \mu}{\partial y}(L,t) = 0, \quad t > 0, \tag{69}$$

$$\mu(y,0) = f_0, \quad \forall y \in [0,L] \tag{70}$$

$$u(y,0) = 0 \quad \forall y \in [0,L]. \tag{71}$$

where f_0 is the external force applied on the sample.
Note that the following equation holds:

$$\sigma = (2\mu_s + \lambda_s)\frac{\partial u}{\partial y} + \sigma_0 - p = -f_0. \tag{72}$$

Thus,

$$\frac{\partial u}{\partial y} = \frac{\mu - f_0}{2\mu_s + \lambda_s + RT\Gamma C_1}. \tag{73}$$

Substitute above relation into (65) gives:

$$\frac{\partial \mu}{\partial t} = (2\mu_s + \lambda_s + RT\Gamma C_1)K\frac{\partial^2 \mu}{\partial y^2}. \tag{74}$$

And its analytical solution is:

$$\mu(y,t) = \frac{4(\mu_0 - f_0 - C_0)}{\pi}\sum_{n=0}^{\infty}\frac{1}{2n+1}\sin\left[\frac{\pi(2n+1)x}{2L}\right]\exp\left[-\frac{K(2\mu_s + \lambda_s + RT\Gamma C_1)\pi^2(2n+1)^2 t}{4L^2}\right]. \tag{75}$$

the solution for u at $y = L$ is calculated according to (73):

$$u(L,t) = \frac{1}{2\mu_s + \lambda_s + RT\Gamma C_1} \int_0^L (\mu(y,t) - f_0)dy \tag{76}$$

5. Simulation results and discussion

We simulated the consolidation experiment using Lanir model by both MHFEM and analytical solution. The table of parameters can be found below:

Table 1. Parameters

Parameter	Unit	Value
$2\mu_s + \lambda_s$	MPa	4×10^3
K	$m^4\ N^{-1}\ s^{-1}$	1.0×10^{-18}
c_0^{fc}	$mol\ m^{-3}$	-2×10^2
c_{out}	$mol\ m^{-3}$	1×10^2
φ_0		0.2
R	$J\ mol^{-1}\ K^{-1}$	8.3145
T	K	293
Γ		0.9
L	m	1
f_0	N	5

5.1. MHFEM simulation

In MHFEM, we use a 2D configuration to simulate the 1D consolidation experiment by tying the nodes which share the same y coordinates together and only allow them to have vertical displacement. In our simulation we use 10 elements in the vertical direction and the time span is $t \in [0, 1000]$ with each time step chosen as 5 seconds.

5.2. Analytical solution

We also plot analytical solutions for both chemical potential and displacement field using the same spacial and time discretization as in the MHFEM simulation.

5.3. Results compare

To compare the simulation results, we typically choose to plot the displacement field and the chemical potential at $y = L$ (where the piston apply the force) in order to observe the maximum change in values. we expect to observe the dropping of the displacement and the increase of the chemical potential from 0 to f_0 (after long enough time).

We compare the result from MHFEM simulation and analytical solution in terms of chemical potential (Fig.2.(a)) and displacement at $y = L$ (Fig.2.(a)) as shown in Fig.2.

5.4. Discussion

From Fig.2, we can conclude that the simulation results fits the analytical solution pretty good at all the time steps which suggests that the MHFEM engine is indeed a reliable computational tool which can be used in the future to describe complex mechanical behaviour of gels besides the 1D consolidation experiment.

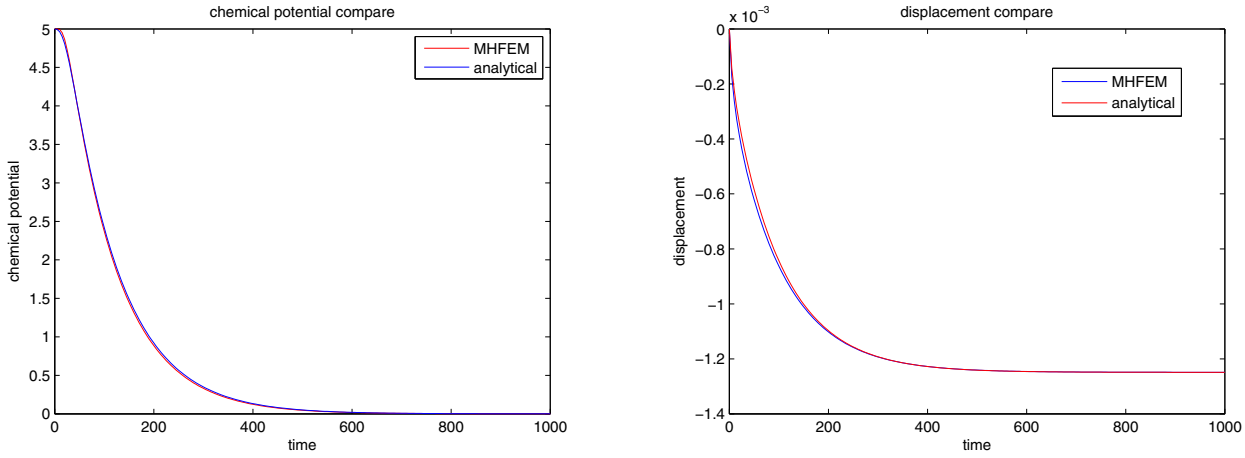

Fig. 2. (a) Chemical potential compare at $y = L$; (b) Displacement compare at $y = L$

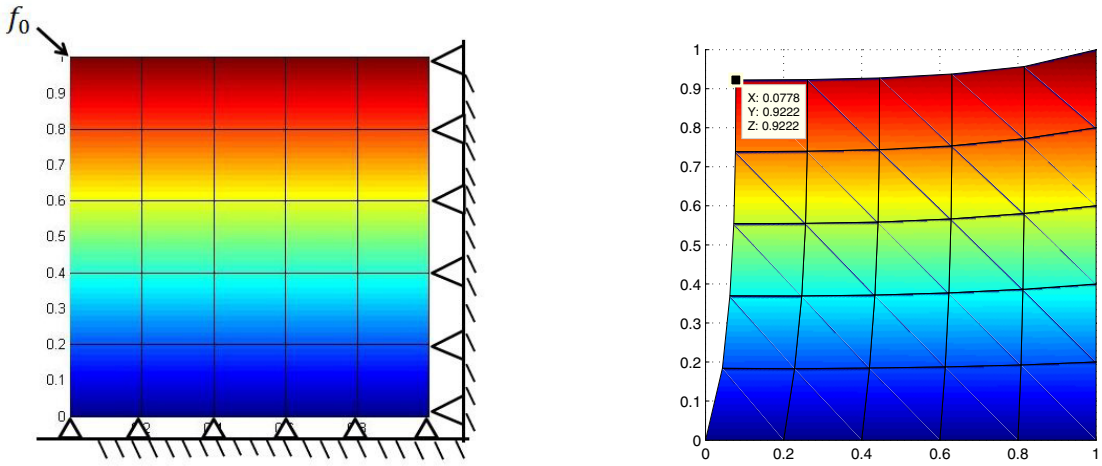

Fig. 3. Point load at the left-up corner (a) Configuration illustration(b) Compressed result

6. Consolidation in two dimensions

To illustrate that the mixed hybrid FEM method presented so far can be easily applied to 2D problems, a 2D consolidation simulations is carried out in a similar fashion. Fig.3 is the simulation result where we apply a point load at the up-left nodes of a square shaped gel with 45 degree angle with he right and bottom boundaries are fixed and the bottom boundary is in contact with outer solution.

We observe symmetric deformation (in x and y direction) from our simulation result, which can be perfectly explained by the symmetric of the force application and the domain configuration.

Acknowledgements

The authors acknowledge the financial support from the Technology Foundation STW, the technological branch of the Netherlands Organization of Scientific Research and the Ministry of Economic Affairs.

References

1. Bowen, R.M.. Incompressible porous media models by use of the theory of mixtures. *International Journal of Engineering Science* 1980; **18**(9):1129–1148.
2. Biot, M.A.. General theory of three-dimensional consolidation. *Journal of applied physics* 1941;**12**(2):155–164.
3. Lanir, Y.. Biorheology and fluid flux in swelling tissues. i. bicomponent theory for small deformations, including concentration effects. *Biorheology* 1986;**24**(2):173–187.
4. Lai, W., Hou, J., Mow, V.. A triphasic theory for the swelling and deformation behaviors of articular cartilage. *Journal of biomechanical engineering* 1991;**113**(3):245–258.
5. Huyghe, J., Janssen, J.. Thermo-chemo-electro-mechanical formulation of saturated charged porous solids. *Transport in Porous Media* 1999;**34**(1-3):129–141.
6. Gu, W., Lai, W., Mow, V.. A mixture theory for charged-hydrated soft tissues containing multi-electrolytes: passive transport and swelling behaviors. *Journal of biomechanical engineering* 1998;**120**(2):169–180.
7. Van Loon, R., Huyghe, J., Wijlaars, M., Baaijens, F.. 3d fe implementation of an incompressible quadriphasic mixture model. *International Journal for Numerical Methods in Engineering* 2003;**57**(9):1243–1258.
8. Van Meerveld, J., Molenaar, M., Huyghe, J., Baaijens, F.. Analytical solution of compression, free swelling and electrical loading of saturated charged porous media. *Transport in porous media* 2003;**50**(1-2):111–126.
9. Wilson, W., Van Donkelaar, C., Huyghe, J.M.. A comparison between mechano-electrochemical and biphasic swelling theories for soft hydrated tissues. *Journal of biomechanical engineering* 2005;**127**(1):158–165.
10. Malakpoor, K., Kaasschieter, E.F., Huyghe, J.M.. Mathematical modelling and numerical solution of swelling of cartilaginous tissues. part ii: Mixed-hybrid finite element solution. *ESAIM: Mathematical Modelling and Numerical Analysis* 2007;**41**(04):679–712.